Chemistry–A European Journal
Research Article
doi.org/10.1002/chem.202302273
Chemistry Europe
European Chemical Societies Publishing
www.chemeurj.org

Special Collection

# Bis(*N*-Heterocyclic Carbene) Manganese(I) Complexes in Catalytic *N*-Formylation/*N*-Methylation of Amines Using Carbon Dioxide and Phenylsilane

Chiara Masaro,[a, b] Giammarco Meloni,[a, c] Marco Baron,[a, c] Claudia Graiff,[d] Cristina Tubaro,*[a, c] and Beatriz Royo*[b]

A series of six Mn(I) complexes with general formula [MnBr(bisNHC)(CO)$_3$], having a bidentate bis(*N*-heterocyclic carbene) ligand (bisNHC), has been developed by varying the bridging group between the NHC donors, the nitrogen wingtip substituents and the heterocyclic ring. The synthesis of the complexes has been accomplished by *in situ* transmetalation of the bisNHC from the corresponding silver(I) complexes. Removal of the bromide anion affords the corresponding solvento complexes [Mn(bisNHC)(CO)$_3$(CH$_3$CN)](BF$_4$). The influence of the bisNHC structure on its electron donor ability has been evaluated by FTIR and $^{13}$C NMR spectroscopy, both in the neutral and cationic complexes. Finally, the isolated Mn(I)-bisNHC complexes have been employed as homogeneous catalysts in the reductive *N*-formylation and *N*-methylation of amines with $CO_2$ as C1 source and phenylsilane as reducing agent, showing a high selectivity for the *N*-methylated product. Preliminary mechanistic investigations suggest that, in the adopted reaction conditions, the formylated product can be formed via different reaction pathways, either metal-catalyzed or not, while the methylation reaction requires the use of the Mn(I) catalyst.

## Introduction

The reductive formylation and methylation of amines using $CO_2$ as C1 building block,[1,2] are two reactions belonging to the so-called diagonal approach for $CO_2$ valorization, which involves reactions combining in a single step the reduction of $CO_2$ and the formation of novel C–X bonds (X = C, N, O).[3,4] The reductive formylation of amines was reported for the first time in 2012 by Cantat and coworkers and can be achieved both by an organometallic- or organo-catalytic process.[4] The reductive methylation of amines is a more challenging reaction, considering that formally consists in a six electrons reduction of the $CO_2$ carbon atom. Furthermore, the latter reaction can create added value, considering the high market value of methylamines.[5] As recently reviewed by Das and coworkers,[6] after the first report by the group of Beller on ruthenium(II)-catalyzed methylation of amines with carbon dioxide and phenylsilane,[7] also Zn(II),[8] Fe(II),[9] Ni(II)[10] and Rh(I)[11] metal complexes, as well as organic compounds, have shown to catalyze this transformation.[12] Moreover, catalyst free versions of the reaction have also been reported, using dimethyl formamide (DMF) or ionic liquids as solvents.[13,14] Up to now there is only one report on Mn-catalyzed reductive methylation of amines with $CO_2$, which describes the use of [Mn$_2$(CO)$_{10}$] in the presence of phosphine ligands as selective catalyst for the double *N*-formylation of aryl amines with phenylsilane.[15]

In this work, we present the first example of a Mn(I)-phosphine free catalytic system for the reductive *N*-formylation and methylation of anilines with $CO_2$, using bidentate NHCs as supporting ligands. In recent years, several studies appeared in the literature regarding the properties of Mn complexes with *N*-heterocyclic carbene (NHC) ligands,[16] and also the number of reports on their application as homogeneous catalysts rapidly increased.[17,18] This is the results of the renaissance of the organometallic chemistry of Earth-abundant metals,[19–21] which takes advantage of the higher availability and the metal precursor's low price, the high bio-compatibility of these metals, and finally their capability of undergoing single electron transfer (SET) processes.[19] Manganese-NHC complexes have been

[a] C. Masaro, G. Meloni, Dr. M. Baron, Prof. Dr. C. Tubaro
Dipartimento di Scienze Chimiche
Università degli Studi di Padova
via Marzolo 1, 35131 Padova (Italy)
E-mail: cristina.tubaro@unipd.it
[b] C. Masaro, Prof. Dr. B. Royo
ITQB NOVA, Instituto de Tecnologia Química e Biológica António Xavier
Universidade Nova de Lisboa
Avenida da República, 2780-157 Oeiras (Portugal)
E-mail: broyo@itqb.unl.pt
[c] G. Meloni, Dr. M. Baron, Prof. Dr. C. Tubaro
CIRCC-Consorzio Interuniversitario per le reattività chimiche e la catalisi, Unità di Padova
Università degli Studi di Padova
Padova (Italy)
[d] Prof. Dr. C. Graiff
Dipartimento di Scienze Chimiche, della Vita e della Sostenibilità Ambientale
Università degli Studi di Parma
Parco Area delle Scienze 17/A, 43124, Parma (Italy)

Supporting information for this article is available on the WWW under https://doi.org/10.1002/chem.202302273
This manuscript is part of a joint special collection on Manganese Homogeneous Catalysis.

reported in a variety of oxidation states namely Mn(0), Mn(I), Mn(II), Mn(III), Mn(IV) and Mn(V), being NHC–Mn(I) the most represented compounds.[16]

As disclosed by some of us, Mn(I) complexes with bisNHC ligands of general formula $[MnBrL(CO)_3]$ (L = bisNHC), are particularly effective in hydrosilylation reactions of aldehydes, ketones, esters, and sulfoxides.[17,22–27] In the hydrosilylation of aliphatic and aromatic aldehydes and ketones with phenylsilane, Mn(I)-bisNHC complexes performed favorably compared to the bypiridyl derivative, indicating that the presence of an NHC unit improves the catalytic performance. Notably, the Mn-catalyzed hydrosilylation of aldehydes, ketones and esters can be performed by using polymethylhydrosilane (PMHS), a cheap and largely available chemical, being a byproduct of the silicone industry.[23,26]

In this work, we prepared a series of new Mn(I) complexes with bidentate bisNHC ligands, whose steric and electronic properties were modulated by varying the length of the linker between the two NHC donors, the nature and hindrance of the wingtip substituents and the type of NHC moiety (see Figure 1 for the ligand precursors[28–30]). The isolated Mn(I)-bisNHC complexes have been employed as well-defined homogeneous catalysts in the reductive formylation and methylation of *N*-ethyl aniline, selected as model substrate.

## Results and Discussion

### Synthesis and Characterization of the Neutral Complexes of General Formula $[MnBr(bisNHC)(CO)_3]$

Complexes **2a** and **2c** were already reported in the literature[26,31,32] and they were synthesized by reacting at 60 °C the proper bis(imidazolium) salt with $[MnBr(CO)_5]$ in the presence of KO$^t$Bu in THF as solvent. While we were submitting our manuscript a paper from Beller and co-workers appeared, reporting the synthesis also of complexes **2b**, **2d** and **2e**, prepared by refluxing (bisNHC)-$BEt_3$ adducts (previously isolated by reaction of the bis(imidazolium) dibromide salts with NaHMDS followed by addition of $BEt_3$) with $[MnBr(CO)_5]$ in THF.[33] In the present work we set up a different procedure, which involves the transmetalation of the dicarbene ligand from the corresponding silver(I) complex (Scheme 1). The advantages of our procedure, compared to the previous one using a strong base (KOBu$^t$), are the milder reaction conditions (lower temperature) and superior yields. In all cases, the coordination of the ligand was confirmed by the disappearance of the C2–H at ca. 9.50 ppm in the $^1$H NMR spectrum and the presence of the characteristic carbene carbon signal around 188–204 ppm in the $^{13}$C NMR spectrum (Table 1). Besides, upon coordination, the hydrogens of the methylene linker connecting the carbene units become diastereotopic, giving an AB or an AA'XX' system, when one or two methylene groups are respectively present. This supports the chelating coordination of the dicarbene ligand to Mn(I), with a slow interconversion of the 6- or 7-membered metallacycle. The ESI-MS (positive mode) spectra show a peak associable to the loss of the bromide ligand from the complex $[M–Br]^+$, in addition to its solvated $CH_3CN$ species $[M–Br + CH_3CN]^+$. The IR spectra corroborates the facial configuration for the tricarbonyl complexes, with the typical presence of three strong bands for the CO stretching (Table 1).

The symmetrical CO stretching vibrations of the complexes allow to find trends in the donating ability of the carbene ligand (Figure 2), comparing bisNHC ligands with different substituents, bridge or heterocyclic rings.

As expected, ligands with aryl wingtips, such as **2c** have a lower donor character compared to NHCs bearing alkyl groups (Me, **2a**; Bn, **2d**). In addition, as expected, imidazol-ylidene moieties have higher donor abilities compared to benzimidazol-ylidene ones; this is attributed to the presence of a condensed aromatic ring, allowing delocalisation of electron density far away from the carbene carbon. It has also been observed that longer bridge linkers increase the electron donor strength of the NHC ligand.[29,35–37] The same trend could be envisaged also

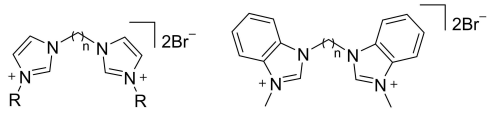


**1a**, n=1, R=Me
**1b**, n=2, R=Me
**1c**, n=1, R=Mes
**1d**, n=1, R=Bn

**1e**, n=1
**1f**, n=2

**Figure 1.** BisNHC ligand precursors used in this study.

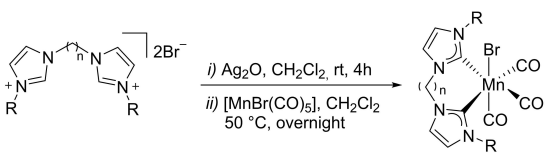


**2a**, n=1, R=Me
**2b**, n=2, R=Me
**2c**, n=1, R=Mes
**2d**, n=1, R=Bn
**2e**, n=1, R=Me, benzimidazol-based NHC
**2f**, n=2, R=Me, benzimidazol-based NHC

**Scheme 1.** General procedure for the synthesis of Mn(I) complexes **2a**–**2f**.

**Table 1.** Selected NMR and IR data of Mn(I) complexes **2a**–**2f**.

| Complex | FT-IR ν(CO) ($cm^{-1}$) | $^{13}$C NMR $\delta_{carbene}$ (ppm) |
|---|---|---|
| **2a** | 2004, 1912, 1881 | 189.3[a] |
| **2b** | 1993, 1887, 1874 | 188.7[b] |
| **2c** | 2007, 1925, 1887 | 191.6[a] |
| **2d** | 2003, 1925, 1886 | 190.5[a] |
| **2e** | 2009, 1925, 1887 | 207.0[b] |
| **2f** | 2001, 1912, 1883 | 201.3[b] |
| $[MnBr(CO)_3(NHC\text{-}CH_2\text{-}py)]$[c] | 2014, 1925, 1882 | 188.1[a] |
| $[MnBr(CO)_3(bpy)]$ | 2027, 1927, 1924 | – |

[a] $^{13}$C NMR spectra registered in DMSO-$d_6$. [b] $^{13}$C NMR spectra registered in $CD_2Cl_2$. [c] Complex $[MnBr(CO)_3(NHC\text{-}CH_2\text{-}py)]$ was already reported in ref.[34]

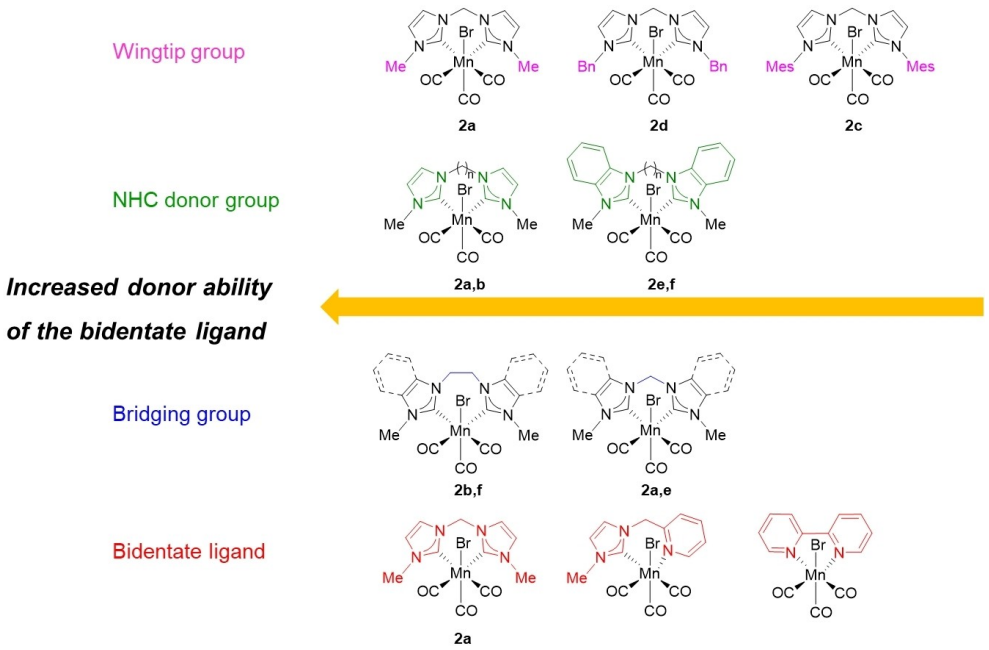


**Figure 2.** Donor ability of the bidentate ligands: trends by changing substituents, bridge, heterocyclic rings or donor atoms.

looking at the signal of the carbene carbon in the $^{13}C$ NMR spectra (Table 1). Finally, the bipyridine ligand has the lowest donor character, which is not surprising considering that the pyridine group possesses a lower donor character than NHCs.

Crystals of complexes **2d** and **2e** were obtained by slow diffusion of diethyl ether into a dichloromethane solution. Single-crystal X-ray diffraction analysis confirmed the octahedral structure of the two complexes (Figure 3). The Mn–$C_{carbene}$, Mn–$C_{carbonyl}$ and Mn–Br bond lengths are in agreement with those of previously reported complexes.[31,32,38,39] Mn–$C_{carbonyl}$ bond distances for carbonyl ligands in plane with the bisNHC ligand are slightly shorter than the Mn–$C_{carbonyl}$ bond length of the carbonyl ligand opposite to the bromide ligand. This reflects the higher *trans* effects of the NHC ligand than the bromide one. In both cases the metallacycle formed by the chelating ligand adopts a boat conformation, thus justifying the diastereotopic nature of the methylene hydrogens of the bridge observed in the $^{1}H$ NMR spectra. The $C_{carbene}$–Mn–$C_{carbene}$ angle (83.5° and 85.5° for **2d** and **2e** respectively) are comparable to those of complexes **2a** (85.11°)[31] and **2c** (83.87°).[32]

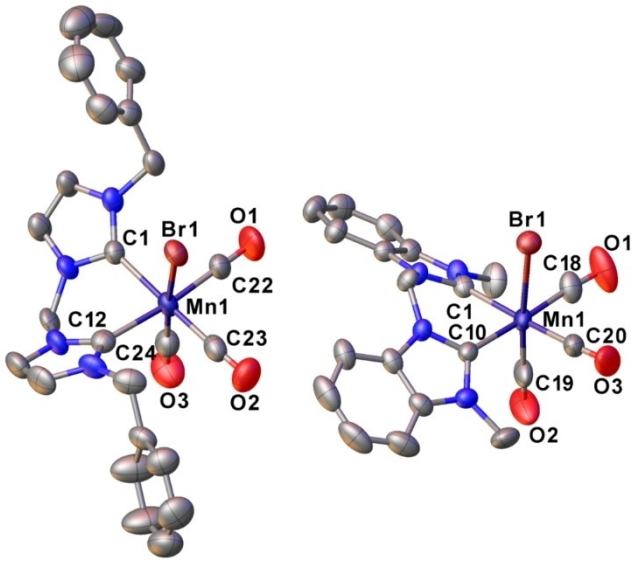


**Figure 3.** ORTEP views of complexes **2d** (left) and **2e** (right) using 50% probability level ellipsoids. List of the most representative bond distances (Å) and angles (°). **2d**: Mn1-C1, 2.050(7); Mn1–C12, 2.052(8); Mn1–C22, 1.81(1); Mn1–C23, 1.803(9); Mn1–C24, 1.773(9); Mn1–Br1, 2.582(1); C1–Mn1–C12, 83.5(3). **2e**: Mn1–C1, 2.037(3); Mn1–C10, 2.026(2); Mn1–C18, 1.814(3); Mn1–C19, 1.784(3); Mn1–C20, 1.816(4); Mn1–Br1, 2.5807(6); C1–Mn1–C10, 85.5(1).

### Synthesis and Characterization of the Cationic Complexes of General Formula [Mn(bisNHC)($CH_3CN$)($CO)_3$]($BF_4$)

The tricarbonyl Mn(I) complexes were converted into their cationic species by abstraction of the bromide ligand with silver tetrafluoroborate in acetonitrile, forming the corresponding [Mn(bisNHC)($CH_3CN$)($CO)_3$]($BF_4$) solvento complexes (Scheme 2).[26] This new family of cationic complexes was synthesized with the aim of having a labile coordination site on the metal center, available for substrate coordination in the catalytic essays. It is expected that the substitution of the acetonitrile solvent molecule will be easier that the substitution of the bromide ligand. We limit this study to the $CH_2$-linker complexes, which are more stable than the ethylene-bridge one, and for which the number of possible conformers is limited.[33]

The success of the reaction was easily appreciated with either NMR or FTIR spectra. In the FTIR spectrum, a new strong and broad peak appears between 1000 and 1100 $cm^{-1}$

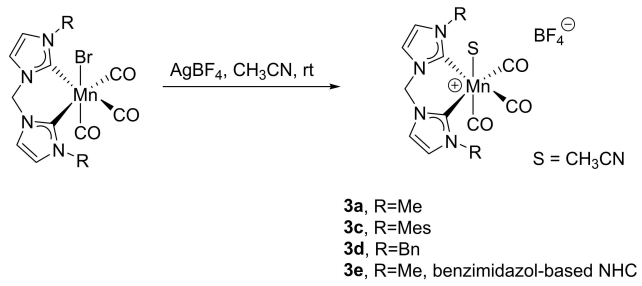


**Scheme 2.** General procedure for the synthesis of the cationic Mn(I) complexes [Mn(bisNHC)($CH_3CN$)$(CO)_3$]($BF_4$) **3a**, **c**, **d**, **e**.

associated to the $BF_4^-$ stretching modes. As expected, carbonyl bands shift to higher wavenumbers due to the lower electron density on the metal center after the bromide abstraction (usually 20 $cm^{-1}$). Within the series of manganese cationic complexes, the same trend of electron donor ability of the bidentate ligand, discussed in the neutral series, is maintained. In the $^1H$ NMR spectrum, the signals appear slightly shifted and the distance between two doublets of the AB system, associated to the methylene linker, is smaller. ESI-MS analysis was not diagnostic, since it showed the same peaks of the pristine neutral complexes, because, in the latter series, the loss of the bromide ligand was observed during ionization. The isolation of cationic complexes was verified for complex **3e** also via X-ray crystal structure analysis. Crystals of **3e** were obtained by slow diffusion of diethyl ether into a solution of the compound in acetonitrile. The single crystal X-ray diffraction analysis confirmed the presence of the acetonitrile coordinated to the manganese (Figure 4). The geometry of the complex is octahedral and the Mn–C bonds are slightly longer than those observed in the pristine neutral complex **2e**, as effect of the positive charge on the metal centre.

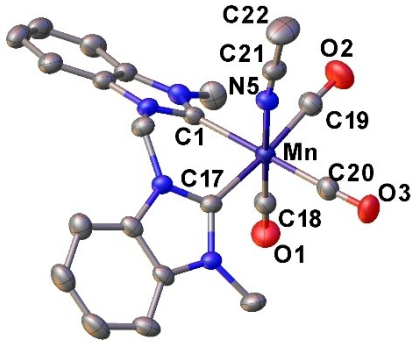


**Figure 4.** ORTEP diagram of the complex **3e** using 50% probability level ellipsoids. Hydrogen atoms, $BF_4$ anion and a disordered acetonitrile solvent molecule are omitted for clarity. List of the most representative bond distances (Å) and angles (°). Mn–C1, 2.050(4); Mn–C17, 2.034(5); Mn–C18, 1.792(5); Mn–C19, 1.845(6); Mn–C20, 1.821(4); Mn–N5, 2.037(3); C1–Mn–C17, 84.6(2).

## Catalytic Results in the Reductive Formylation/Methylation of amines

The catalytic activity of selected manganese(I) bisNHC complexes was studied in the reductive formylation and methylation of *N*-ethylaniline with $CO_2$ (Scheme 3). For the benchmark reaction, to evaluate the different activity of these Mn complexes, the *N*-ethylaniline was used as substrate, carrying out the reaction at 5 atm $CO_2$ pressure, 80 °C, in acetonitrile solution, using phenylsilane (3 equivalents) as reducing agent.

Whilst in the benchmark conditions the blank experiment gave no conversion of the reagent (Table 2, entry 1), the neutral manganese(I) complexes show moderate catalytic efficiencies. The bisNHC ligand is important in influencing the catalytic performance of the manganese(I) complex: all the tested [$MnBr(CO)_3$(bisNHC)] complexes (Table 2, entries 2–6) outperformed the complex with the bipyridine ligand, [$MnBr(CO)_3$(bpy)], or the Mn(I) precursor [$MnBr(CO)_5$] (Table 2, entries 9 and 10). Complex [$MnBr(CO)_3$(NHC-$CH_2$-Py)] presents instead a higher conversion of the amine (Table 2, entry 8), although with a preference towards the less interesting *N*-formyl product **5a**. The selectivity among the two possible products appears influenced by the ligand as well. The formylation product is prevalent in most cases, however with complex **2c**, bearing methylene-bridged imidazol-2-ylidene donors with mesityl wingtips the *N*-methylation product is the main one, whereas with complex **2f**, bearing ethylene-bridged benzymidazol-2-ylidene donors with methyl wingtips, the two

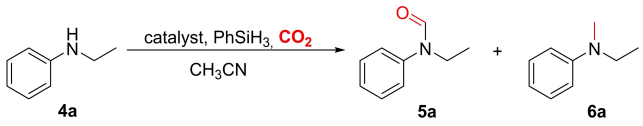


**Scheme 3.** Methylation/formylation of *N*-ethylaniline to the *N*-formylated (**5a**) and the *N*-methylated (**6a**) products.

**Table 2.** Performance of the Mn(I) complexes in formylation/methylation of *N*-ethylaniline **4a**.[a]

| Entry | Catalyst | Conversion (%) | **5a** (%) | **6a** (%) |
|---|---|---|---|---|
| 1 | – | 0 | 0 | 0 |
| 2 | **2a** | 48 | 34 | 14 |
| 3 | **2c** | 40 | 14 | 26 |
| 4 | **2d** | 42 | 31 | 11 |
| 5 | **2e** | 24 | 23 | 1 |
| 6 | **2f** | 55 | 26 | 29 |
| 7 | **3d** | 31 | 22 | 9 |
| 8 | [$MnBr(CO)_3$(NHC-$CH_2$-Py)] | 64 | 52 | 12 |
| 9 | [$MnBr(CO)_3$(bpy)] | 6 | 6 | 0 |
| 10 | [$MnBr(CO)_5$] | 8 | 8 | 0 |

[a] Reaction conditions: catalyst 1% mol, *N*-ethylaniline **4a** (0.4 mmol, 1 equiv), $PhSiH_3$ (1.2 mmol, 3 equiv), $CH_3CN$ (1 mL), T = 80 °C, $p_{CO2}$ = 5 atm, t = 7 h, yields determined by $^1H$ NMR using 2,5-dimethylfuran as an internal standard.

products are obtained in comparable yields. Complex **2b**, having an ethylene linker and imidazole-2-ylide NHC units, was not tested since it appears rather unstable in solution for prolonged times. The cationic complex **3d** shows slightly lower conversion than the corresponding neutral complex **2d** (Table 2, entries 4 and 7), thus suggesting that the preliminary removal of the bromido ligand is not necessary since it can occur in the catalytic mixture.[31]

The effect of the temperature and of the catalyst loading on the reaction outcome is known to be a significant aspect.[15,40] As reported by Cantat and coworkers, the high temperature allows the hydrosilylation of formamides to take place, thus favoring the conversion of the *N*-formyl product into the *N*-methyl one.[9] For this reason, we performed some test on the benchmark reaction at different catalyst loading and temperature (Table 3) using prevalently complex **2a** as catalyst. The reaction time was prolonged to 20 h in order to reach higher conversions of the amine and a better selectivity towards the methylated product, whose formation is more interesting and more difficult to be achieved.

Complex **2a** in 1 mol% at 80 °C affords full conversion of the amine (Table 3, entry 2). The selectivity towards the methylated product grows with the catalyst amount, but also with the temperature (compare for example entries 2 and 3, or entries 5, 6 and 7 in Table 3). As matter of fact, using 5% catalyst load at 100 °C the yield in the methylated product increases up to 58% using complex **2a** (Table 3, entry 7). Gratifyingly, the yield of product **6a** can be increased to 82% by increasing the amount of $PhSiH_3$ up to 6 equivalents (Table 3 entry 8). We have performed the same catalytic experiment reported in Table 3, entry 7 also with a different catalyst, complex **2c** (Table 3, entry 9), that showed a better selectivity toward the methylated product **6a** even at lower temperature and catalysts loading (Table 2, entry 3). This trend was confirmed also at higher temperature and catalyst loading (Table 3, entry 8), obtaining 80% yield in **6a**. However, in this case, by increasing the quantity of $PhSiH_3$ up to 6 equiv., the yield in **6a** only slightly increased (entry 10, Table 3).

**Table 3.** Complex **2a** activity in formylation/methylation of *N*-ethylaniline at different temperatures and catalyst load.[a]

| Entry | 2a (mol%) | T (°C) | Conversion (%) | **5a** (%) | **6a** (%) |
|---|---|---|---|---|---|
| 1 | – | 80 | – | – | – |
| 2 | 1 | 80 | 100 | 80 | 20 |
| 3 | 2.5 | 80 | 100 | 65 | 35 |
| 4 | – | 100 | 41 | 32 | 9 |
| 5 | 1 | 100 | 100 | 75 | 25 |
| 6 | 2.5 | 100 | 100 | 50 | 50 |
| 7 | 5 | 100 | 100 | 42 | 58 |
| 8 | 5[b] | 100 | 100 | 18 | 82 |
| 9 | 5[c] | 100 | 100 | 20 | 80 |
| 10 | 5[b,c] | 100 | 100 | 15 | 85 |

[a] Reaction conditions: catalyst **2a**, *N*-ethylaniline **4a** (0.2 mmol, 1 equiv.), $PhSiH_3$ (0.6 mmol, 3 equiv.), $CH_3CN$ (1 mL), $p_{CO2}$ = 5 atm, t = 20 h. Conversion and yields determined by $^1H$ NMR using 2,5-dimethylfuran as internal standard. [b] Test performed using 0.2 mmol of **4a** and 1.2 mmol, 6 equiv. of $PhSiH_3$. [c] Test performed by using catalyst **2c** instead of **2a**.

It is worth noting that the blank test (in the absence of Mn catalyst) performed at 100 °C afforded a 41% substrate conversion in 20 h (Table 3, entry 4), yielding 32% of **5a** and only 9% of **6a**. It is known that polar organic solvents can promote the methylation and formylation of amines with $CO_2$, as reported for example in the case of dimethylformamide (DMF) and dimethylsulfoxide (DMSO). This behavior is attributed to the ability of such solvents to promote the reactivity of the Si–H bond with $CO_2$ through solvation and polarization effects.[13,41] Moreover, in the blank experiment (Table 3, entry 4) product **6a** is formed in low yield (9%), this is again in agreement with the studies reported by Lei and coworkers, stating that the catalyst free methylation of amines with $PhSiH_3$ does not follow a stepwise reaction pathway through the formylated product (**5a** in this case). The methylated product yield increases in fact in the presence of the catalyst (9% catalyst free, 25, 50 and 58% with 1, 2.5 and 5 mol% of Mn complex, respectively).

We decided therefore to have more information on the mechanism of the metal catalyzed reaction, with the aim of a better tuning of the catalytic conditions and further improving the selectivity of the reaction. In this frame it is important to remark that the reaction mechanism is still under debate and can be different for different catalysts. In general, the formation of the *N*-methyl product is supposed to occur stepwise, via the reduction of the *N*-formyl compound.[7,8] However, in few cases it is reported that the formation of the *N*-formyl and *N*-methyl products follow two distinct reaction pathways and the further reduction of the *N*-formyl product does not take place.[13,40] In our experiments using catalyst **2a**, it was found, analyzing the reaction mixture at the end of a catalytic test by $^1H$ NMR in $CDCl_3$, that together with the desired products, a clearly detectable amount of formic acid was obtained (Figure S21). Formic acid is likely formed upon hydrolysis of silylformate, thus indicating that in the presence of the Mn(I) catalysts used in this work, the formation of the products proceed via the silylformate route, as previously reported by Cantat and Beller.[7,8] Moreover, it has also been reported that *N*-formylation and *N*-methylation of amines can be performed by reacting the amine with formic acid and hydrosilanes in the presence of a catalyst.[42–44] This possibility was evaluated also in our catalytic system. As shown in Scheme 4, the reaction of *N*-ethylaniline with formic acid, in the presence of $PhSiH_3$ and **2a** (5 mol%) at 100 °C leads to the complete substrate conversion, with the


**Scheme 4.** Formylation and methylation of *N*-ethylaniline with formic acid. Reaction conditions: *N*-ethylaniline (0.081 mmol), HCOOH (0.243 mmol), $PhSiH_3$ (0.243 mmol), **2a** (0.0043 mmol), 100 °C. 20 h. NMR yields of **5a** and **6a** reported in parentheses.

formation of **5a** and **6a** in a 3/2 ratio. A blank experiment was also carried out in the same conditions but without **2a**, affording again the complete substrate conversion, although with the selective formation of only **5a**. The formylation of amines with formic acid was indeed described by different authors.[45–47] It seems however clear that the methylated product **6a** could not be formed from formic acid in the absence of complex **2a**. We also carried out the reaction of formic acid (1 equiv.) and phenylsilane (1 equiv.) in the presence of catalyst **2a** (5 mol%), heating the mixture at 80 °C for 2 h in $CD_3CN$. Most likely, this reaction would produce hydrogen and the corresponding silylformate. In the $^1$H-NMR spectrum we observed the presence of $H_2$, the disappearance of the signal of formic acid and the broadening of the signals in the aromatic region. Then, if *N*-ethylaniline (1 equiv.) is added and the mixture is heated at 80 °C for further 16 h, full conversion of the *N*-ethylaniline and formation of a mixture **5a**/**6a** in approximately 1/1 ratio was observed.

Then, in order to verify if the formation of the *N*-methyl product occurs via the reduction of the *N*-formyl compound, we have performed the experiment showed in Scheme 5, where we tried to convert *N*-methylformanilide **5b** into *N*,*N*-dimethylaniline **6b**, using $PhSiH_3$ and catalyst **2a** in $CD_3CN$ at 100 °C. After 13 h, **5b** was completely converted in **6b**, indicating that complex **2a** can catalyze the process. We also run a blank experiment in the same conditions but without **2a**, observing no reaction. Finally, the mixture **5a**/**6a**, obtained at the end of the catalytic reaction reported in Table 3, entry 8, was treated with $PhSiH_3$ (6 equiv.) and fresh catalyst (5 mol%), and the reaction was heated at 80 °C for further 20 h. In this way, full conversion of the residual *N*-ethylformanilide **5a** into the *N*-methylated product **6a** was obtained. These findings mark a relevant difference with other catalytic systems reported in the literature. For example, Xia and coworkers reported that the $[CpFe(CO)_2]_2/PPh_3$,[40] cannot convert *N*-ethylformanilide **5a** into *N*-ethyl-*N*-methylaniline **6a** under conditions very closed to those adopted in Scheme 5.

The whole of these experiments suggests that in our case the formylated product can be formed via three different reaction pathways, i.e. i) polar solvents promoted or ii) metal catalyzed reaction between the amine with $CO_2$ and $PhSiH_3$, ii) metal catalyzed reaction between the amine and formic acid, formed by hydrolysis of silylformate generated *in situ* by reaction of $CO_2$ and $PhSiH_3$. On the other hand, the methylated product should be formed mainly by Mn-catalyzed reduction with $PhSiH_3$ of the formyl derivative. The amount of $PhSiH_3$ appears therefore crucial in determining the selectivity of the reaction, since it participates directly in both processes. Considering that the performance of the catalyst could also be influenced by the employed amine, we performed a screening of the reaction using different secondary amines using **2a** as catalyst (5 mol%) at 100 °C for 20 h and 6 equiv. of $PhSiH_3$. With all substrates full amine conversion was observed with the product distribution reported in Table 4. With *N*-methylaniline the product distribution strongly resembles the one obtained with *N*-ethylaniline (entries 1 and 2, Table 4). By introducing electron-withdrawing (4-$NO_2$) or electron-donating (4-MeO) groups on the aryl ring of aniline the product distribution changes (entries 3 and 4 Table 4). The methylated product **6c** is the only one observed in the case of electron withdrawing (4-$NO_2$) group, whereas with electron-donating group (4-MeO) the ratio between products **5d** and **6d** is close to 4:6. The reaction proceeds smoothly also with dibenzyl amine, affording the methylated product **6e** in good yield. In the case of the cyclic aliphatic amines piperidine, the formamide **5f** was formed selectively (entry 6, Table 4).

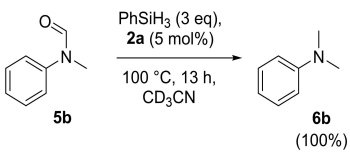


**Scheme 5.** Reduction of *N*-methylformanilide **5b** to *N*,*N*-dimethylaniline **6b**. Reaction conditions: **5b** (0.081 mmol), $PhSiH_3$ (0.243 mmol), **2a** (0.004 mmol), 100 °C, 13 h, $CD_3CN$ (1 mL).

**Table 4.** Formylation/methylation of different amines using catalyst **2a**.[a]

| Entry | Substrate | Products (yield %) | |
|---|---|---|---|
| 1 | 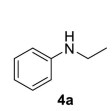 **4a** | 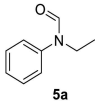 **5a** (18) | 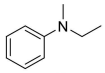 **6a** (82) |
| 2 |  **4b** |  **5b** (23) |  **6b** (77) |
| 3 | 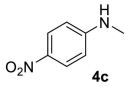 **4c** | 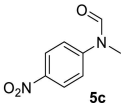 **5c** (n.d.) | 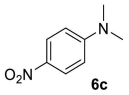 **6c** (94) |
| 4 | 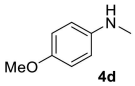 **4d** | 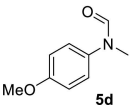 **5d** (37) | 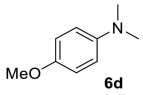 **6d** (63) |
| 5 | 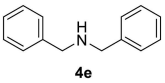 **4e** | 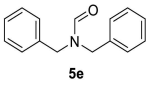 **5e** (30) | 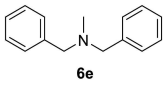 **6e** (70) |
| 6 |  **4f** | 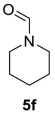 **5f** (96) | 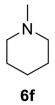 **6f** (n.d.) |

[a] Reaction conditions: Amine (0.33 mmol), **2a** (5 mol%), $PhSiH_3$ (6 eq), $CH_3CN$ (1 mL), $p_{CO2}$ = 5 atm, t = 20 h. Yields determined by $^1$H NMR using 2,5-dimethylfuran as internal standard.

## Conclusions

In summary, we have synthesized and fully characterized two series of neutral and cationic manganese complexes of general formula [MnBr(bisNHC)(CO)$_3$] and [Mn(CH$_3$CN)(bisNHC)(CO)$_3$](BF$_4$), respectively. The complexes differ for the steric and electronic properties of the bisNHC ligand, which are in agreement with the trend expected on the basis of *N*-wingtip substituent, the length of the linker between the two NHC heterocyclic rings and the NHC-based ring. Preliminary results on Mn-NHC-catalyzed *N*-methylation and *N*-formylation of anilines using $CO_2$ as C1 source and phenylsilane as reducing agent are reported. Complex **2a** resulted an efficient catalyst for the *N*-methylation of several amines using $CO_2$ and phenylsilane. Furthermore, the catalytic data show that while the formylated product can be obtained using a free-catalytic system, the methylation reaction requires the use of a metal-based catalyst in the adopted reaction conditions. Moreover, considering the variety of complexes isolable with the silver transmetalation of the carbene ligand, we are exploring other possible catalytic application for this class of compounds.

## Experimental Section

All the syntheses of the manganese complexes were performed under a nitrogen atmosphere using standard Schlenk techniques and the manipulation of the complexes was carried out under reduced light conditions. Solvents for syntheses were dried according to published methods and distilled before use. Bis(azolium) salts were synthesized according the literature procedures.[28–30,48] [MnBr(CO)$_5$] was purchased from Strem chemicals and used as received. $^1$H and $^{13}$C NMR spectra were recorded on a Bruker Avance III 400 MHz (operating at 400.1 MHz for $^1$H and 101 MHz for $^{13}$C) or on a Bruker Avance 300 MHz (operating at 300.1 MHz for $^1$H and 75.5 MHz for $^{13}$C). Electrospray mass spectra (ESI-MS) were provided by the laboratories at ITQB.

### General procedure for the synthesis of the neutral manganese(I) complexes [MnBr(bisNHC)(CO)$_3$]

In a Schlenk tube, the bis(carbene) proligand (1 eq) was suspended in dry dichloromethane, followed by $Ag_2O$ (1.2 eq) addition, and the resulting mixture was stirred for 4 h at room temperature under inert atmosphere. The manganese precursor [MnBr(CO)$_5$] (1 eq) was then added, and the suspension stirred overnight at 50 °C. After cooling to room temperature, the suspension was filtered through a pad of Celite and the obtained solution was concentrated to dryness under vacuum. The residue was washed with $Et_2O$ three times to afford the desired product.

**2a**. Yellow solid (yield 63%). The characterization of the complex is in accord with data previously reported for **2a** prepared by a different procedure.[31]

**2b**. Yellow solid (yield 81%). $^1$H NMR ($CD_2Cl_2$, 400 MHz, 25 °C) δ (ppm): 4.15 (s, 6H, $CH_3$), 4.51 (dd, $J$ = 15.1 Hz, 8.2 Hz, 2H, $NCH_2$), 5.05 (dd, $J$ = 15.1 Hz, 8.2 Hz, 2H, $NCH_2$), 6.95 (s, 2H, $CH_{im}$), 7.02 (s, 2H, $CH_{im}$). $^{13}$C{$^1$H} NMR ($CD_2Cl_2$, 100 MHz, 25 °C) δ (ppm): 40.7 ($NCH_3$), 50.5 ($NCH_2$), 123.2 ($C_{im}$), 124.86 ($C_{im}$), 188.7 ($C_{carbene}$), 220.1 (CO), 222.8 (CO). IR (KBr): 1993 (s), 1887 (s), 1874 (s) cm$^{-1}$. The characterization of the complex is in accord with data previously reported for **2b** prepared by a different procedure.[33] We have included the $^{13}$C{$^1$H} NMR data that was not reported before.

**2c**. Light brown solid (yield 77%). The characterization of the complex is in accord with data previously reported for **2a** prepared by a different procedure.[32]

**2d**. Yellow powder (yield 90%). $^1$H NMR (DMSO, 400 MHz, 25 °C) δ (ppm): 5.60 (d, $J$ = 15.2 Hz, 2H, $NCH_2C$), 5.75 (d, $J$ = 15.2 Hz, 2H, $NCH_2C$), 6.10 (d, $J$ = 12.9 Hz, 1H, $NCH_2N$), 6.67 (d, $J$ = 12.9 Hz, 1H, $NCH_2N$), 7.14 (s, 2H, $CH_{im}$), 7.25 (m, 4H, $CH_{o\text{-}Ar}$), 7.32 (m, 2H, $CH_{p\text{-}Ar}$), 7.38 (m, 4H, $CH_{m\text{-}Ar}$), 7.62 (s, 2H, $CH_{im}$). $^{13}$C{$^1$H} NMR (DMSO, 100 MHz, 25 °C) δ (ppm): 53.1 ($NCH_2C$), 61.8 ($NCH_2N$) 122.2 ($CH_{im}$), 122.7 ($CH_{im}$), 127.4 ($C_{o\text{-}Ar}$), 127.7 ($C_{p\text{-}Ar}$), 128.6 ($C_{m\text{-}Ar}$), 137.2 ($C_{i\text{-}Ar}$), 190.5 ($C_{carbene}$), 219.6 (CO). IR (KBr): 2003 (s), 1925 (s), 1886 (s) cm$^{-1}$. HR-ESI-MS (positive mode): *m/z* 508.1175 [*M*-Br + CH$_3$CN]$^+$ calculated for $C_{26}H_{23}N_5O_3Mn^+$ = 508.1181, 467.0908 [*M*-Br]$^+$ calculated for $C_{24}H_{20}N_4O_3Mn^+$ = 467.0916. Crystals of **2d** were obtained by slow diffusion of diethyl ether into a solution of the complex in dichloromethane. The characterization of the complex is the same reported in the literature for the same complex isolated with a different procedure.[33] We have included the $^{13}$C{$^1$H} NMR data that was not reported before.

**2e**. Yellow solid (yield 90%). $^1$H NMR (DMSO, 400 MHz, 25 °C) δ (ppm): 4.25 (s, 6H, $NCH_3$), 6.74 (br, 1H, $NCH_2$), 7.25 (d, $J$ = 13.1 Hz, 1H, $NCH_2$), 7.44 (m, 4H, $CH_{bim}$), 7.73 (d, $J$ = 7.7 Hz, 2H, $CH_{bim}$), 8.25 (d, $J$ = 7.7 Hz, 2H, $CH_{bim}$ $^1$H NMR ($CD_2Cl_2$, 300 MHz, 25 °C) δ (ppm): 4.28 (s, 6H, $NCH_3$), 6.47 (d, $J$ = 13.1 Hz, 1H, $NCH_2$), 7.26 (br, 1H, $NCH_2$), 7.39 (m, 4H, $CH_{bim}$), 7.48 (d, $J$ = 7.7 Hz, 2H, $CH_{bim}$), 7.62 (d, $J$ = 7.7 Hz, 2H, $CH_{bim}$). $^{13}$C{$^1$H} NMR ($CD_2Cl_2$, 75 MHz, 25 °C) δ (ppm): 35.3 ($NCH_3$), 56.0 ($NCH_2N$), 108.9 ($CH_{bim}$), 110.7 ($CH_{bim}$), 123.7 ($CH_{bim}$), 123.9 ($CH_{bim}$), 134.0 ($C_{bim}$), 136.1 ($C_{bim}$), 207.0 ($C_{carbene}$), 220.2 (CO). IR (KBr): 2009 (s), 1925 (s), 1887 (s) cm$^{-1}$. HR-ESI-MS (positive mode): *m/z* 456.0861 [*M*-Br + CH$_3$CN]$^+$ calculated for $C_{22}H_{19}N_5O_3Mn^+$ = 456.0868, 415.0592 [*M*-Br]$^+$ calculated for $C_{20}H_{16}N_4O_3Mn^+$ = 415.0603. Crystals of **2e** were isolated by slow diffusion of diethyl ether into a dichloromethane solution of the complex. The characterization of the complex is the same reported in the literature for the same complex isolated with a different procedure.[33] We have included the $^{13}$C{$^1$H} NMR data that was not reported before.

**2f**. Yellow powder (yield 50%). $^1$H NMR ($CD_2Cl_2$, 400 MHz, 25 °C) δ (ppm): 4.37 (s, 6H, $NCH_3$), 4.90 (dd, 1H, $J$ = 15.0, 8.2 Hz, $NCH_2$), 5.63 (dd, $J$ = 15.0, 8.2 Hz, 1H, $NCH_2$), 7.37 (m, 4H, $CH_{bim}$), 7.45 (m, 4H, $CH_{bim}$). $^{13}$C{$^1$H} NMR ($CD_2Cl_2$, 100 MHz, 25 °C) δ (ppm): 36.8 ($NCH_3$), 45.9 ($NCH_2$), 109.5 ($CH_{bim}$), 110.6 ($CH_{bim}$), 123.5 ($CH_{bim}$), 123.8 ($CH_{bim}$), 135.6 ($C_{bim}$), 136.4 ($C_{bim}$), 201.3 ($C_{carbene}$), carbonyl signals not detected. IR (KBr): 2001 (s), 1912 (s), 1883 (s) cm$^{-1}$.

### General procedure for the synthesis of the cationic manganese(I) complexes [Mn(bisNHC)(CH$_3$CN)(CO)$_3$](BF$_4$)

The proper neutral complex [MnBr(bisNHC)(CO)$_3$] (1 eq) was dissolved in acetonitrile (15 mL) and $AgBF_4$ (1.1 eq) was then added. The resulting suspension was stirred at room temperature overnight. Then, the reaction mixture was filtered on Celite and the solvent was removed under vacuum to afford the desired compound.

**3a**. Off-white solid (yield 71%). The characterization of **3a** is in accord with data reported in the literature.[26]

**3c**. Brown solid (yield 46%). $^1$H NMR ($CD_3CN$, 400 MHz, 25 °C) δ (ppm): 1.87 (s, 6H, $CH_{3Ar}$), 2.06 (s, 6H, $CH_{3Ar}$), 2.31 (s, 6H, $CH_{3Ar}$), 6.17 (d, J = 13.5 Hz, 1H, $NCH_2N$), 6.28 (d, J = 13.5 Hz, 1H, $NCH_2N$), 7.01 (s, 2H, $CH_{Ar}$), 7.04 (s, 2H, $CH_{Ar}$), 7.15 (s, 2H, $CH_{im}$), 7.67 (s, 2H, $CH_{im}$). IR

(KBr): 2021(s), 1939 (s), 1923 (s) $cm^{-1}$. HR-ESI-MS (positive mode): 564.1805 $[M\text{-}BF_4]^+$ calculated for $C_{30}H_{31}N_5O_3Mn^+ = 564.1808$.

**3 d**. Yellow solid (yield 55 %). $^1H$ NMR ($CD_3CN$, 400 MHz, 25 °C) δ (ppm): 5.51 (d, $J = 16.1$ Hz, 2H, $NCH_2C$), 5.61 (d, $J = 16.1$ Hz, 2H, $NCH_2C$), 6.14 (d, $J = 13.9$ Hz, 1H, $NCH_2N$), 6.29 (d, $J = 13.9$ Hz, 1H, $NCH_2N$), 7.06 (s, 2H, $CH_{im\text{-}4}$), 7.12 (d, $J = 7.4$ Hz, 4H, $CH_{Ar}$), 7.36 (m, 6H, $CH_{Ar}$), 7.51 (s, 2H, $CH_{im\text{-}5}$). $^{13}C\{^1H\}$ NMR ($CD_3CN$, 100 MHz, 25 °C) δ (ppm): 54.2 ($NCH_2C$), 63.5 ($NCH_2N$), 123.8 ($CH_{im\text{-}4}$), 124.4 ($CH_{im\text{-}5}$), 127.8 ($C_{o\text{-}Ar}$), 128.8 ($C_{p\text{-}Ar}$), 129.8 $C_{m\text{-}Ar}$), 137.9 ($C_{i\text{-}Ar}$), 189.5 ($C_{carbene}$), 217.7 (CO). IR (KBr): 2019 (s), 1944 (s), 1924 (s) $cm^{-1}$. HR-ESI-MS (positive mode): 508.1180 $[M\text{-}BF_4]^+$ calculated for $C_{26}H_{23}N_5O_3Mn^+ = 508.1181$.

**3 e**. Off-white solid (yield 96 %). $^1H$ NMR ($CD_3CN$, 300 MHz, 25 °C) δ (ppm): 4.18 (s, 6H, $NCH_3$), 6.47 (d, $J = 14.0$ Hz, 1H, $NCH_2$), 6.81 (d, $J = 14.0$ Hz, 1H, $NCH_2$), 7.48 (m, 4H, $CH_{bim}$), 7.64 (d, $J = 7.2$ Hz, 2H, $CH_{bim}$), 7.94 (d, $J = 7.2$ Hz, 2H, $CH_{bim}$). $^{13}C$ NMR ($CD_3CN$, 75 MHz, 25 °C) δ (ppm): 35.4 ($NCH_3$), 57.0 ($NCH_2N$), 110.8 ($CH_{bim}$), 111.8 ($CH_{bim}$), 124.8 ($CH_{bim}$), 134.8 ($C_{bim}$), 136.5 ($C_{bim}$), 202.2 ($C_{carbene}$), carbonyl signals not detected. IR (KBr): 2026(s), 1947 (s), 1914 (s) $cm^{-1}$. HR-ESI-MS (positive mode): 456.0867 $[M\text{- }BF_4]^+$ calculated for $C_{22}H_{19}N_5O_3Mn^+ = 456.0868$. Crystals of complex **3 e** were obtained by slow diffusion of ether in an acetonitrile solution.

### General procedure for reductive N-formylation and N-methylation of amines with $CO_2$

The catalytic experiments were carried out in a Fisher-Porter type reactor. The solid catalyst was introduced into the tube, then 0.5 mL of acetonitrile were added, obtaining a solution. Next, a precise quantity of the amine (substrate) and $PhSiH_3$ were added. Finally, 0.5 mL more of acetonitrile were added washing carefully the tube walls. The reactor was subsequently closed tightly and 5 cycles of pressurization/depressurization with $CO_2$ were performed. The reactor was pressurized with 5 atm of $CO_2$ and dipped into a thermostatic bath. The stirring speed and immersion depth were maintained similar in all the performed tests. The starting time of the test was defined 5 minutes after the immersion of the reaction tube in the thermostatic bath. At the end of the test the reactor was removed from the thermostatic bath, cooled to room temperature using a water bath, and depressurized to ambient pressure. The reactor was then opened, and a precise quantity of internal standard (2,5-dimethylfurane) was added. The obtained solution was then mixed, and a small sample of the reaction mixture was transferred into an NMR tube and the $^1H$ NMR spectrum in $CDCl_3$ was registered. A tiny amount of solid $K_2CO_3$ can be added to the NMR tube to have a better spectrum. Products yield can be obtained from the ratio of the normalized areas of selected signals of the products and of the standard. The identification of products was performed by comparison of the $^1H$ NMR spectra with the spectra reported in the literature (see Supporting Information).

### X-Ray structure determination of complexes 2 d, 2 e and 3 e

Crystals suitable for single-crystal X-ray analysis for complexes **2 d** and **2 e** were selected, covered with Fomblin (polyfluoro ether oil) and mounted on a nylon loop. The data were collected at room temperature on a Bruker D8 Venture diffractometer equipped with a Photon 100 CMOS detector, using graphite monochromated Mo–Kα radiation (λ = 0.71073 Å). The data were processed using the APEX3 suite software package, which includes integration and scaling (SAINT), absorption corrections (SADABS[49]) and space group determination (XPREP). Structure solution and refinement were done using direct methods with the programs SHELXT 2014/5 and SHELXL-2018/3[50,51] inbuilt in APEX and WinGX-Version 2021.3[52] software packages. All non-hydrogen atoms were refined anisotropically and the hydrogen atoms were inserted in idealized positions and allowed to refine riding on the parent carbon atom. The crystallographic data for complex **3 e** were obtained by mounting a single crystal on a glass fiber and transferring it to an APEX II Bruker CCD diffractometer. The APEX 3 program package was used to obtain the unit-cell geometrical parameters and for the data collection (30s/frame scan time for a sphere of diffraction data). The raw frame data were processed using SAINT and SADABS to obtain the data file of the reflections. The structures were solved using SHELXT[53] (Intrinsic Phasing method in the APEX 3 program). The refinement of the structures (based on $F^2$ by full-matrix least-squares techniques) was carried out using the SHELXTL-2014/7 program.[50] The hydrogen atoms were introduced in the refinement in defined geometry and refined "riding" on the corresponding carbon atoms. The molecular diagrams were drawn with Olex2.[54] Crystal data and refinement parameters are reported in Table S1.[55]

## Supporting Information

The authors have cited additional references within the Supporting Information.[56–62]

## *Acknowledgements*

This work was supported by the Department of Chemical Sciences of the University of Padova [P-DiSC#01BIRD2019-UNIPD, PI: M. Baron] and by Fundação para a Ciência e Tecnologia (FCT) for Projects PTDC/QUI-QIN/0359/2021, MOST-MICRO-ITQB, UDIB/04612/2020, and UIPD/04612/2020. The National NMR Facility is supported by CERMAX through Project 022162. C. Almeida and UniMS facility at ITQB NOVA are acknowledged for HRMS. The authors would like to thank the Crystallography Service of the LAQV, Department of Chemistry, NOVA School of Science and Technology, Portugal, for the structural determination of the complexes **2 d** and **2 e**.

## *Conflict of Interests*

The authors declare no conflict of interest.

## *Data Availability Statement*

The data that support the findings of this study are available in the supplementary material of this article.

**Keywords:** bidentate ligands · carbon dioxide valorization · manganese(I) complexes · methylation of amines · *N*-heterocyclic carbene

[1] G. Naik, N. Sarki, V. Goyal, A. Narani, K. Natte, *Asian J. Org. Chem.* **2022**, *11*, e202200270.
[2] V. Goyal, G. Naik, A. Narani, K. Natte, R. V. Jagadeesh, *Tetrahedron* **2021**, *98*, 132414.

[3] C. Das Neves Gomes, O. Jacquet, C. Villiers, P. Thuéry, M. Ephritikhine, T. Cantat, *Angew. Chem. Int. Ed.* **2012**, *51*, 187–190.
[4] O. Jacquet, C. Das Neves Gomes, M. Ephritikhine, T. Cantat, *J. Am. Chem. Soc.* **2012**, *134*, 2934–2937.
[5] Q. Liu, L. Wu, R. Jackstell, M. Beller, *Nat. Commun.* **2015**, *6*, 5933.
[6] Y. Zhang, T. Zhang, S. Das, *Green Chem.* **2020**, *22*, 1800–1820.
[7] Y. Li, X. Fang, K. Junge, M. Beller, *Angew. Chem. Int. Ed.* **2013**, *52*, 9568–9571.
[8] O. Jacquet, X. Frogneux, C. D. N. Gomes, T. Cantat, *Chem. Sci.* **2013**, *4*, 2127–2131.
[9] X. Frogneux, O. Jacquet, T. Cantat, *Catal. Sci. Technol.* **2014**, *4*, 1529–1533.
[10] L. González-Sebastián, M. Flores-Alamo, J. J. García, *Organometallics* **2015**, *34*, 763–769.
[11] R. H. Lam, C. M. A. McQueen, I. Pernik, R. T. McBurney, A. F. Hill, B. A. Messerle, *Green Chem.* **2019**, *21*, 538–549.
[12] a) S. Das, F. D. Bobbink, G. Laurenczy, P. J. Dyson, *Angew. Chem. Int. Ed.* **2014**, *53*, 12876–12879; b) M. Hulla, G. Laurenczy, P. J. Dyson, *ACS Catal.* **2018**, *8*, 10619–10630.
[13] H. Niu, L. Lu, R. Shi, C.-W. Chiang, A. Lei, *Chem. Commun.* **2017**, *53*, 1148–1151.
[14] X.-Y. Li, S.-S. Zheng, X.-F. Liu, Z.-W. Yang, T.-Y. Tan, A. Yu, L.-N. He, *ACS Sustainable Chem. Eng.* **2018**, *6*, 8130–8135.
[15] Z. Huang, X. Jiang, S. Zhou, P. Yang, C.-X. Du, Y. Li, *ChemSusChem* **2019**, *12*, 3054–3059.
[16] S. M. P. Vanden Broeck, C. S. J. Cazin, *Polyhedron* **2021**, *205*, 115204.
[17] S. Friães, S. Realista, H. Mourão, B. Royo, *Eur. J. Inorg. Chem.* **2022**, *2022*, e202100884.
[18] G. Meloni, L. Beghetto, M. Baron, A. Biffis, P. Sgarbossa, M. Mba, P. Centomo, L. Orian, C. Graiff, C. Tubaro, *J. Mol. Catal.* **2023**, *538*, 113006.
[19] M. Albrecht, R. Bedford, B. Plietker, *Organometallics* **2014**, *33*, 5619–5621.
[20] J. Loup, U. Dhawa, F. Pesciaioli, J. Wencel-Delord, L. Ackermann, *Angew. Chem. Int. Ed.* **2019**, *58*, 12803–12818.
[21] S. Rana, J. Prasad Biswas, S. Paul, A. Paik, D. Maiti, *Chem. Soc. Rev.* **2021**, *50*, 243–472.
[22] S. C. A. Sousa, C. J. Carrasco, M. F. Pinto, B. Royo, *ChemCatChem* **2019**, *11*, 3839–3843.
[23] S. C. A. Sousa, S. Realista, B. Royo, *Adv. Synth. Catal.* **2020**, *362*, 2437–2443.
[24] M. F. Pinto, M. Olivares, Á. Vivancos, G. Guisado-Barrios, M. Albrecht, B. Royo, *Catal. Sci. Technol.* **2019**, *9*, 2421–2425.
[25] S. Friães, S. Realista, C. S. B. Gomes, P. N. Martinho, L. F. Veiros, M. Albrecht, B. Royo, *Dalton Trans.* **2021**, *50*, 5911–5920.
[26] M. Pinto, S. Friães, F. Franco, J. Lloret-Fillol, B. Royo, *ChemCatChem* **2018**, *10*, 2734–2740.
[27] H. Mourão, C. S. B. Gomes, S. Realista, B. Royo, *Appl. Organomet. Chem.* **2022**, 10.1002/aoc.6846.
[28] C. Tubaro, A. Biffis, R. Gava, E. Scattolin, A. Volpe, M. Basato, M. M. Díaz-Requejo, P. J. Perez, *Eur. J. Org. Chem.* **2012**, *2012*, 1367–1372.
[29] A. Volpe, A. Sartorel, C. Graiff, M. Bonchio, A. Biffis, M. Baron, C. Tubaro, *J. Organomet. Chem.* **2020**, *917*, 121260.
[30] F. A. Westerhaus, B. Wendt, A. Dumrath, G. Wienhöfer, K. Junge, M. Beller, *ChemSusChem* **2013**, *6*, 1001–1005.
[31] F. Franco, M. F. Pinto, B. Royo, J. Lloret-Fillol, *Angew. Chem. Int. Ed.* **2018**, *57*, 4603–4606.
[32] Y. Yang, Z. Zhang, X. Chang, Y.-Q. Zhang, R.-Z. Liao, L. Duan, *Inorg. Chem.* **2020**, *59*, 10234–10242.
[33] N. F. Both, A. Spannenberg, H. Jiao, K. Junge, M. Beller, *Angew. Chem. Int. Ed.* **2023**, *62*, 10.1002/anie.202307987.
[34] M. Huang, Y. Li, Y. Li, J. Liu, S. Shu, Y. Liu, Z. Ke, *Chem. Commun.* **2019**, *55*, 6213–6216.
[35] G. Buscemi, M. Basato, A. Biffis, A. Gennaro, A. A. Isse, M. M. Natile, C. Tubaro, *J. Organomet. Chem.* **2010**, *695*, 2359–2365.
[36] M. G. Gardiner, C. C. Ho, *Coord. Chem. Rev.* **2018**, *375*, 373–388.
[37] H. V. Huynh, *Chem. Rev.* **2018**, *118*, 9457–9492.
[38] K. Ganguli, A. Mandal, S. Kundu, *ACS Catal.* **2022**, *12*, 12444–12457.
[39] J. Agarwal, T. W. Shaw, C. J. Stanton III, G. F. Majetich, A. B. Bocarsly, H. F. Schaefer III, *Angew. Chem. Int. Ed.* **2014**, *53*, 5152–5155.
[40] W.-D. Li, D.-Y. Zhu, G. Li, J. Chen, J.-B. Xia, *Adv. Synth. Catal.* **2019**, *361*, 5098–5104.
[41] H. Lv, Q. Xing, C. Yue, Z. Lei, F. Li, *Chem. Commun.* **2016**, *52*, 6545–6548.
[42] I. Sorribes, K. Junge, M. Beller, *Chem. Eur. J.* **2014**, *20*, 7878–7883.
[43] L. Zhu, L.-S. Wang, B. Li, W. Li, B. Fu, *Catal. Sci. Technol.* **2016**, *6*, 6172–6176.
[44] C. Genre, I. Benaissa, T. Godou, M. Pinault, T. Cantat, *Catal. Sci. Technol.* **2022**, *12*, 57–61.
[45] C. L. Allen, J. M. J. Williams, *Chem. Soc. Rev.* **2011**, *40*, 3405–3415.
[46] B. A. Aleiwi, K. Mitachi, M. Kurosu, *Tetrahedron Lett.* **2013**, *54*, 2077–2081.
[47] D. Habibi, M. Nasrollahzadeh, H. Sahebekhtiari, *J. Mol. Catal. Chem.* **2013**, *378*, 148–155.
[48] M. Baron, A. Dall'Anese, C. Tubaro, L. Orian, V. Di Marco, S. Bogialli, C. Graiff, M. Basato, *Dalton Trans.* **2018**, *47*, 935–945.
[49] L. Krause, R. Herbst-Irmer, G. M. Sheldrick, D. J. Stalke, *Appl. Cryst.* **2015**, *48*, 3–10.
[50] G. M. Sheldrick, *Acta Crystallogr. Sect. C Struct. Chem.* **2015**, *71*, 3–8.
[51] C. B. Hübschle, G. M: Sheldrick, B. Dittrich, *J. Appl. Crystallogr.* **2011**, *44*, 1281–1284.
[52] L. J. Farrugia, *J. Appl. Crystallogr.* **2012**, *45*, 849–854.
[53] G. M. Sheldrick, *Acta Crystallogr. Sect. Found. Adv.* **2015**, *71*, 3–8.
[54] O. V. Dolomanov, L. J. Bourhis, R. J. Gildea, J. A. K. Howard, H. Puschmann, *J. Appl. Crystallogr.* **2009**, *42*, 339–341.
[55] Deposition Numbers 2281370 (for **2d**), 2281371 (for **2e**), 2281372 (for **3e**) contain the supplementary crystallographic data for this paper. These data are provided free of charge by the joint Cambridge Crystallographic Data Centre and Fachinformationszentrum Karlsruhe Access Structures service.
[56] X.-F. Li, X.-G. Zhang, F. Chen, X.-H. Zhang, *J. Org. Chem.* **2018**, *83*, 12815–12821.
[57] Z. Guo, T. Pang, L. Yan, X. Wei, J. Chao, C. Xi, *Green Chem.* **2021**, *23*, 7534–7538.
[58] J. Tang, J. Kong, H. Xu, Z.-J. Jiang, Y. She, J. Bai, B. Tang, J. Chen, Z. Gao, K. Gao, *J. Org. Chem.* **2023**, *88*, 1560–1567.
[59] G. Li, J. Chen, D.-Y. Zhu, Y. Chen, J.-B. Xia, *Adv. Synth. Catal.* **2018**, *360*, 2364–2369.
[60] A. E. Wahba, M. T. Hamann, *J. Org. Chem.* **2012**, *77*, 4578–4585.
[61] T. A. Gokhale, S. C. Gulhane, B. M. Bhanage, *Eur. J. Org. Chem.* **2023**, *26*, e202200997.
[62] Z. Wang, S. Chen, C. Chen, Y. Yang, C. Wang, *Angew. Chem. Int. Ed.* **2023**, *62*, e202215963.

Manuscript received: July 17, 2023
Accepted manuscript online: September 11, 2023
Version of record online: October 24, 2023